Effects of the Microstructure of Fibrous Media on their Acoustic Properties

C. Peyrega[*,1] and D. Jeulin[1]
[1]Center of Mathematical Morphology, Mathematics and Systems, Mines ParisTech
*Charles Peyrega: [1]Center of Mathematical Morphology, 35 Rue St-Honoré, 77300 Fontainebleau (France), charles.peyrega@cmm.ensmp.fr

Abstract: This study is a part of the Silent Wall[A] ANR project, to which the CMM is associated. Its main objective is to build an acoustic and thermal insulating system for buildings, composed of fibrous materials. As a reference material, the Thermisorel® is composed of two phases: the fibrous network and the air surrounding it. At the microscopic scale the absorption of the acoustic wave is mainly due to viscous and thermal damping into the boundary layer at the interface between fibres and pores. Therefore, fully coupled harmonic compressible flow equations for velocity, pressure and temperature must be solved within the "thermo-acoustics" module of COMSOL Multiphysics. In the framework of homogenization methods into this module, unit cells of 3D periodic arrays of cylindrical fibres are modeled in 2D to study the influence of their size, internal porosity, and thickness on their acoustic properties.

Keywords: Fibrous materials, homogenization, random media, thermo-acoustics.

1. Introduction

The main objective of the Silent Wall project is focused on the optimization of the acoustic properties of fibrous media. For this purpose, our study especially deals with the modeling of the microstructures of such media to estimate the influence of the dimensions of the fibres on their coefficient of absorption. The reference fibrous material for Silent Wall, called Thermisorel®, is made of wooden fibres from a paper-making process.

[A] http://us2b.pierroton.inra.fr/Projets/Silent_Wall/description.htm

2. Equations of thermo-acoustics

2.1 The governing equations

Our problem of thermo-acoustics is described by the following harmonic equations solved for the air considered as a visco-thermal fluid at the microscopic scale. The first one is the equation of Navier Stokes (2), then the equation of continuity (3), the heat equation (4), and finally the equation of the perfect gases (5). These equations are solved for the flow velocity $\vec{U}$, the pressure P and the temperature of the fluid, which are three harmonic variables (1).

$$\vec{U} = \vec{u}e^{i\omega t}; P = P_0 + pe^{i\omega t}; T = T_0 + \tau e^{i\omega t} \quad (1)$$

The fluctuation of velocity is $\vec{u}$, the variations p and τ are respectively called acoustic pressure and temperature. Considering a porous medium of porosity ϕ with a rigid frame, these four equations are solved in the porosity Ω_f saturated by air having a viscosity η, a second viscosity ζ, a density ρ_0, a thermal conductivity κ and a specific heat capacity C_p.

$$i\omega\rho_0\vec{u} = -\vec{\nabla}p + \left(\frac{\eta}{3} + \zeta\right)\vec{\nabla}\left(\vec{\nabla}.\vec{u}\right) + \eta\Delta\vec{u} \quad (2)$$

$$i\omega\frac{\rho}{\rho_0} + \vec{\nabla}.\vec{u} = 0 \quad (3)$$

$$i\omega\rho_0 C_p\tau = \kappa\Delta\tau + i\omega p \quad (4)$$

$$\rho = \rho_0\left(\frac{p}{P_0} - \frac{\tau}{T_0}\right) \quad (5)$$

2.2 The boundary conditions

Let Γ be the fluid-solid interface. Since the solid frame is a rigid wall with no-slip conditions, all velocity components are set to zero. Moreover, this interface is isothermal, which means that T is equal to the ambient temperature T_0 (5).

$$\vec{u}_\Gamma = \vec{0}; \tau_\Gamma = 0 \quad (5)$$

2.3 Multi-scale approach and homogenization

The macroscopic effective acoustic properties of our porous media are estimated by the method of homogenization from periodic unit cells [2,3,16] which was used in several similar studies [6,9,10,11,17]. For this purpose, we assume that the material is equivalent to a homogeneous medium composed of periodic unit cells Ω. Thus the three variables $\vec{u}$, p and τ are Ω-periodic. According to this method the three variables can be expressed from a multi-scale point of view (6). The scale separation parameter $\varepsilon = \frac{l}{L} << 1$ is the ratio between the unit cell length *l* and the characteristic length the acoustic wave *L* (7) [4], with c_0 the speed of sound in the air. The space variables $\vec{y}$ and $\vec{x} = \varepsilon \vec{y}$ respectively characterize the micro-variations and the macro-variations [16].

$$\begin{cases} \vec{u}(\vec{x},\vec{y}) = \overrightarrow{u^{(0)}}(\vec{x},\vec{y}) + \varepsilon \overrightarrow{u^{(1)}}(\vec{x},\vec{y}) + \varepsilon^2 \overrightarrow{u^{(2)}}(\vec{x},\vec{y}) + ... \\ p(\vec{x},\vec{y}) = p^{(0)}(\vec{x},\vec{y}) + \varepsilon p^{(1)}(\vec{x},\vec{y}) + \varepsilon^2 p^{(2)}(\vec{x},\vec{y}) + ... \\ \tau(\vec{x},\vec{y}) = \tau^{(0)}(\vec{x},\vec{y}) + \varepsilon \tau^{(1)}(\vec{x},\vec{y}) + \varepsilon^2 \tau^{(2)}(\vec{x},\vec{y}) + ... \end{cases} \quad (6)$$

$$L = \frac{\lambda_{wave}}{2\pi} = \frac{c_0}{\omega} \quad (7)$$

By restricting the equations (6) to the first order [(0)] into the equations (2-3-4-5), we obtain the following set of equations (8-9-10-11) [2,9,10]. Assuming that viscous and thermal phenomena can be handled separately [1,5,7,8,15]. The generalized Darcy's law can be used to estimate the tensor of dynamic viscous permeability **K** (8), from which we can define both dynamic effective density and viscous tortuosity (9) [1,5,7]. We note $\hat{\boldsymbol{K}} = \phi \langle \boldsymbol{K} \rangle$, with the tensor $\langle \boldsymbol{K} \rangle$ being the spatial average value of **K** into the pores Ω_f.

$$\overrightarrow{u^{(0)}}(\vec{x},\vec{y}) = -\frac{\boldsymbol{K}(\vec{y},\omega)}{\eta} . \vec{\nabla}_x p^{(0)}(\vec{x}) \quad (8)$$

$$\boldsymbol{\rho_{eff}} = \frac{\eta \phi}{i\omega} \hat{\boldsymbol{K}}^{-1} = \boldsymbol{\alpha}(\omega) \rho_0 \quad (9)$$

Handling the thermal phenomena, we obtain the scalar thermal permeability K' (10), and the compressibility modulus χ_{eff} (11) which depends on $\hat{K}' = \phi \langle K' \rangle$.

$$\tau^{(0)}(\vec{x},\vec{y}) = \frac{K'(\vec{y},\omega)}{\kappa} i\omega p^{(0)}(\vec{x}) \quad (10)$$

$$\chi_{eff}(\omega) = \frac{1}{\gamma P_0} \left(\gamma - \left[(\gamma - 1) \frac{\rho_0 \, \mathrm{Pr}}{\eta} \frac{i\omega \hat{K}'}{\phi} \right] \right) \quad (11)$$

Thus, knowing the couple $\left(\hat{\boldsymbol{K}}, \hat{K}'\right)$ is essential to estimate the average acoustic properties of the homogeneous material of thickness *d* and composed of periodic unit cells. Thus, it is possible to estimate the coefficient of absorption (17) of this material with the help of the equations (12-13-14-15-16). Let $\vec{Q}$ (12) be the wave vector defined from the unit vector $\vec{\xi}$. Both effective celerity c_{eff} (13) of the wave into the medium and effective impedance Zc_{eff} (14) can be estimated from the equations (9) and (11).

$$\vec{Q} = Q.\vec{\xi} \quad (12)$$

$$c_{eff} = \frac{\omega}{Q} = \sqrt{\frac{\overrightarrow{\xi^T} . \boldsymbol{\rho_{eff}}^{-1} . \vec{\xi}}{\chi_{eff}}} \quad (13)$$

$$Zc_{eff} = \frac{1}{\phi} \sqrt{\frac{\overrightarrow{\xi^T} . \boldsymbol{\rho_{eff}} . \vec{\xi}}{\chi_{eff}}} \quad (14)$$

Finally, the transfer function H into the medium of thickness *d* (15) and the corresponding coefficient of reflection R(ω) (16) lead to the coefficient of absorption A(ω) (17), with $Z_0 = \rho_0 c_0$ the impedance of the air.

$$H(\omega,d) = \left(\frac{1 + e^{\frac{-2i\omega d}{c_{eff}}}}{1 - e^{\frac{-2i\omega d}{c_{eff}}}} \right) = \coth(iQd) \quad (15)$$

$$R(\omega) = \frac{HZc_{eff} - Z_0}{HZc_{eff} + Z_0} \quad (16)$$

$$A(\omega) = 1 - |R(\omega)|^2 \quad (17)$$

3. Modeling with COMSOL Multiphysics

3.1 Geometries and meshes

To highlight the effects of the dimensions of fibres on their acoustic properties, we chose to model them in 2D into the "thermo-acoustics"

module of COMSOL Multiphysics. Considering a periodic array of fibres with square sections[17] all parallel in 3D (Figure 1), and having a thickness *d* along the direction (here *Ox*) of the wave propagation, it is possible to estimate its acoustic properties from those of the 2D sections of the material in the planes perpendicular to the fibres (here the *xOy* planes).

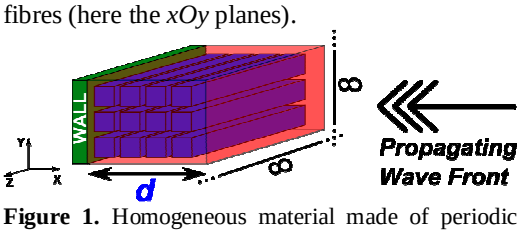

Figure 1. Homogeneous material made of periodic unit cells composed of fibres with square sections. The material has a thickness *d* along the *Ox* axis and infinite thicknesses along both *Oy* and *Oz* axis. The wave front propagates in the *Ox* direction.

Two different types of periodic arrays were studied. The first one is made of plain fibres having a square section (Figure 2), which is called "*2D PASC NO LUMEN*" according to the name "Periodic Array of Square Cylinders" already proposed by Venegas *et al.* in their paper[17] in 2008. We call "lumens" the internal porosity of our reference wooden fibres where the sap of the tree flows. These internal porosities are oriented along the axis of the fibres.

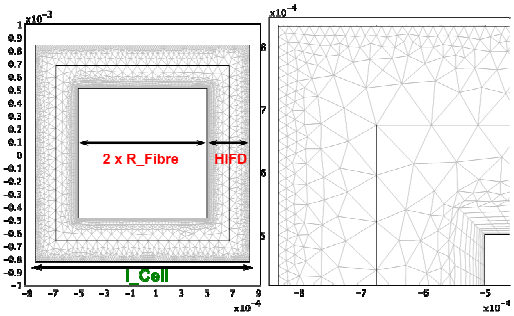

Figure 2. Mesh of the *2D PASC NO LUMEN* geometry.

The second geometry, called "*2D PASC LUMEN*", handles these lumens (Figure 3). For both types of unit cells only the pores around the fibres are meshed. Moreover both meshes are refined at the air-fibre Γ interface to solve more precisely the boundary layer at high frequencies. Since the unit cell is periodic, the meshes are refined at its four boundaries.

Both geometries are defined by the length l_c of the unit cell, the radius of the fibre R_F and by the Half Inter-Fibre Distance (*HIFD*). Moreover, the *2D PASC LUMEN* geometry has an additional parameter: R_{Lumen}, the radius of the internal porosity.

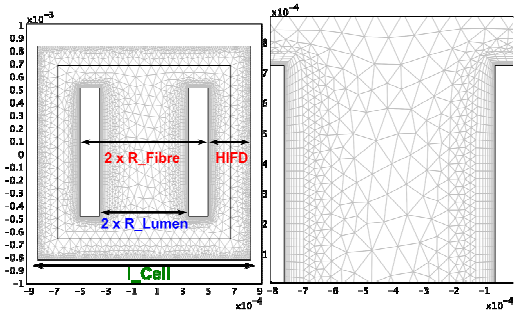

Figure 3. Mesh of the *2D PASC LUMEN* geometry.

The geometries shown in Figures 2 and 3 have a radius R_F equal to $100\mu m$, and an external porosity of *0.64*. The internal porosity of *2D PASC LUMEN* is equal to *0.25*, which makes a total porosity equal to *0.89*. Finally the ratio $\frac{R_{Lumen}}{R_F} = \frac{25}{36}$ is chosen for our porous fibres.

These numerical values describing the microstructural properties of our fibrous materials were previously estimated from morphological analysis of the microstructure in 3D of X Ray-CT images of Thermisorel®[12,13].

3.2 Implementation into COMSOL Multiphysics

In the subdomain composed by the air saturating the pores the harmonic equations (2-3-4-5) are solved. No-slip boundary conditions for the velocity are set at the air-fibre interfaces, which are set isothermal (5). To simulate an acoustic wave propagating in the *Ox* direction from the left to the right, an oscillating acoustic pressure p_{in} (here equal to *1 Pa*) is applied at the left boundary of the unit cell, and no constraints are set on its three other edges. Moreover, periodic boundary conditions are set for all components of $\vec{u}$, and for the fluctuations p and τ on the boundaries of the unit cell.

4. Experimental Results

4.1 Acoustic temperature and boundary layers

Three cases were studied. The first one consisted in stimulating the geometry "*2D PASC NO LUMEN*" in the *Ox* direction (Figure 4). The second one was focused on the response of the geometry "*2D PASC LUMEN*" to an incoming wave oriented in the *Ox* direction, orthogonally to the lumens (Figure 5). And finally the same porous fibres were stimulated in the *Oy* direction along their lumens (Figure 6).

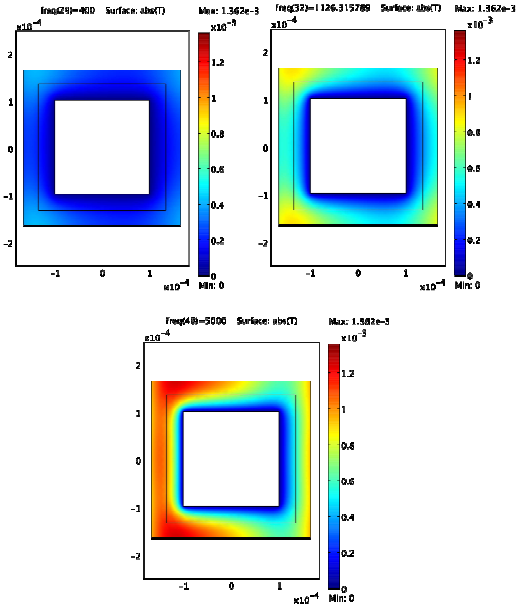

Figure 4. Fields of acoustic temperature τ of the *2D PASC NO LUMEN* geometry stimulated in the Ox direction for f = 400Hz, 1126 Hz and 5000 Hz.

The Figures (4-5-6) are all represented with identical ranges of acoustic temperatures τ for frequencies equal to 400Hz, 1126Hz and 5000Hz. For the three cases a common trend is noticeable: a boundary layer is observable in *blue* at the air-fibre interface. The viscous and thermal dissipation of acoustic energy are located in this boundary layer whose depth δ_{BL} depends on the frequency of the propagating wave according to the equation (18)[1]. Thus, the lower the frequency, the thicker the boundary layer, which is observable on the Figures (4-5-6). On the contrary, at high frequencies the boundary layer tends to disappear.

$$\delta_{BL} = \sqrt{\frac{2\eta}{\omega\rho_0}} = \sqrt{\frac{\eta}{f\pi\rho_0}} \qquad (18)$$

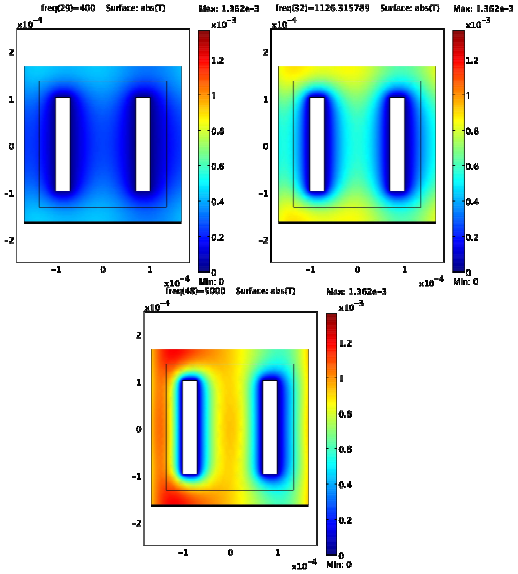

Figure 5. Fields of acoustic temperature τ of the *2D PASC LUMEN* geometry stimulated in the Ox direction for f = 400Hz, 1126 Hz and 5000 Hz.

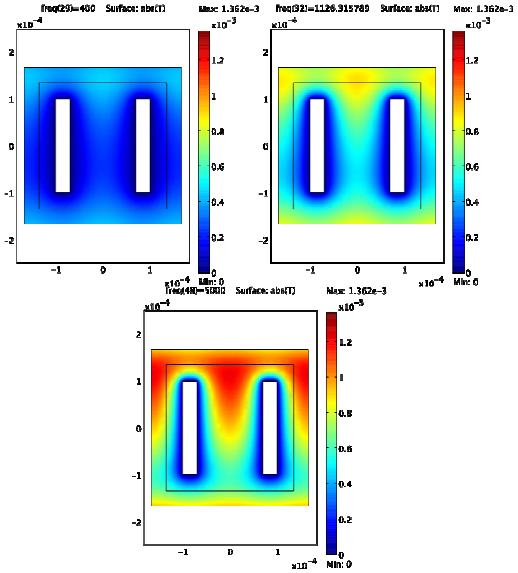

Figure 6. Fields of acoustic temperature τ of the *2D PASC LUMEN* geometry stimulated in the Oy direction for f = 400Hz, 1126 Hz and 5000 Hz.

When the frequencies are too low for the studied geometries (here at f=400Hz for R_F=100µm), the boundary layers of nearby unit cells overlap, which reduces the surface area

where the energy dissipations take place. Thus, the absorption coefficient is reduced when nearby boundary layers overlap.

The diagram in Figure 7 links the radii R_F of the fibres of the *2D PASC NO LUMEN* unit cell to the depth of the boundary layer according to the equation (18). The Figure 7 highlight the frequency evolution of R_F when nearby boundary layers just touch each other, i.e. when δ_{BL}=*HIFD* (*black* plot). Into the *yellow* area, nearby boundary layers overlap, and they are separated in the *purple* zone. Thus from these relations and from the Figure 7 it is possible to define the so-called "Minimum Absorbed Frequency" (MAF) such as frequencies higher than MAF separate the boundary layers and then are properly absorbed by the geometry.

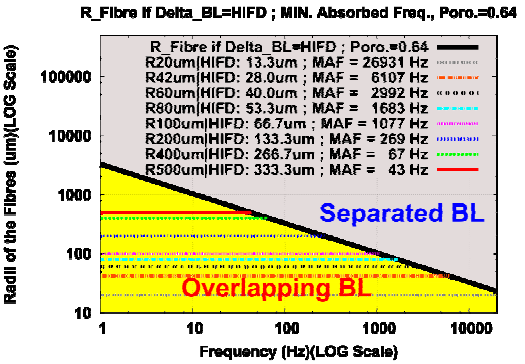

Figure 7. Evolution with the frequency of the radii of the fibres when nearby boundary layers just touch each other (i.e. when δ_{BL}=HIFD) (in black) for the geometry *2D PASC NO LUMEN*. Identification of the domains where nearby BL are separated (in purple) or overlap (in yellow). Estimation of the minimum absorbed frequencies for each radius of fibres.

4.2 Coefficient of absorption and radii of the fibres

To link the acoustic properties of the 2D geometries to the radii of the fibres, both external and internal porosity are constant and respectively set to 0.64 and 0.25. Note that the internal porosity of *2D PASC NO LUMEN* is 0. Thus, the porosities being constant, only R_F is modified by homothetically changing the corresponding geometries into COMSOL Multiphysics. The thickness *d* of the material is set to *2 cm* (Figures 8 and 9).

The Figure 8 compares the coefficients of absorption of both geometries *2D PASC NO LUMEN* (*NL* thin lines) and *2D PASC LUMEN* (*LX* thick lines) stimulated in the *Ox* direction, for a range of frequencies into 0Hz and 5000Hz, and for different radii R_F between 10µm and 500µm. According to the Figure 8, the coefficient of absorption is higher for the porous fibres *2D PASC LUMEN* stimulated orthogonally to their lumens, than for the plain fibres, whatever their radius R_F.

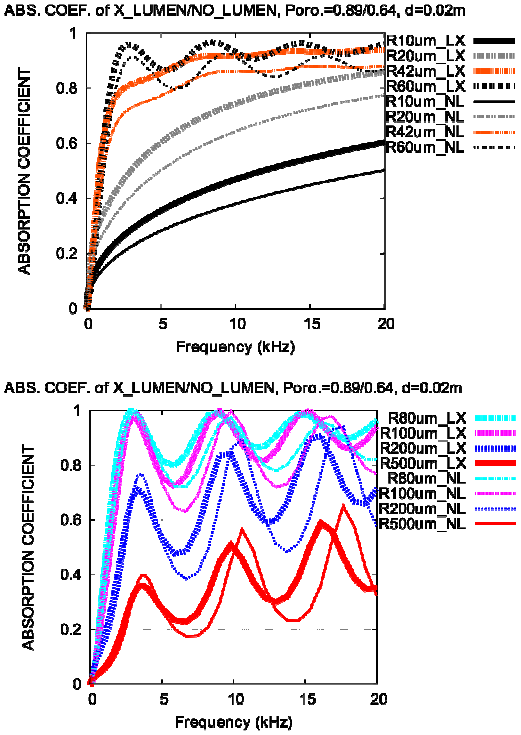

Figure 8. Comparison of the coefficients of absorption of both geometries *2D PASC NO LUMEN* and *2D PASC LUMEN* stimulated in the Ox direction, for different radii of the fibres and for *d=2cm*.

The second point concerns the influence of R_F on A(ω). When R_F gets smaller, the specific surface area of contact between fibres and air increases for the homogeneous material, which lets suppose that small fibres better absorb the acoustic waves. But this assumption is only valid until a certain value of R_F. For both geometries, the coefficient of absorption increases when R_F gets lower from 500µm to 80µm. However the limiting effect of overlapping nearby boundary layers is observable for smaller fibres when R_F

varies from 80µm to 10µm. This can be confronted with the minimum absorbed frequencies of each radius presented in the Figure 7 for the geometry *2D PASC NO LUMEN*.

The Figure 9 focuses on the acoustic performances of the *2D PASC LUMEN* stimulated either orthogonally (*LX* thick lines, in the *Ox* direction), or along the internal porosity (*LY* thin lines, in the *Oy* direction). Considering porous fibres, their absorption coefficient is highly dependent on the direction of stimulation. For larger fibres, the coefficient A(ω) is globally higher for a stimulation orthogonally to the lumens than along them. This trend is reversed for smaller fibres which better absorb the acoustic energy when stimulated along their internal porosity. Moreover, the same observation as for the Figure 8, can be made: the absorption coefficient globally increases when R_F changes from 500µm to 80µm, and then gets lower for smaller radii, due to the overlap of nearby boundary layers.

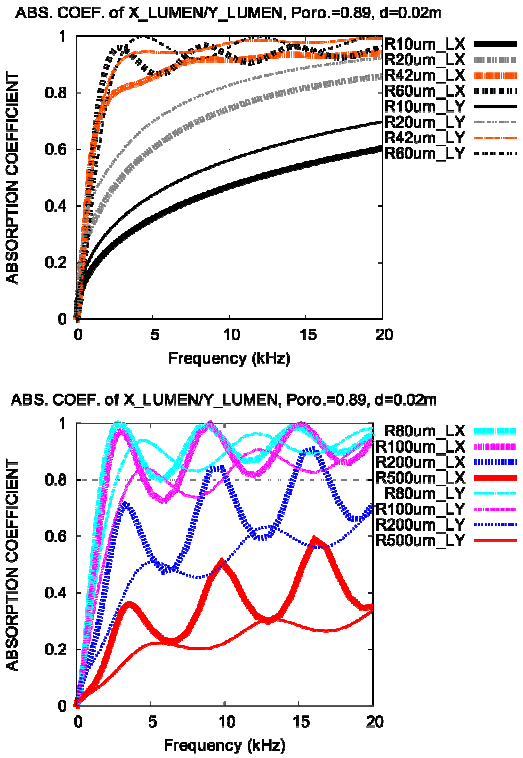

Figure 9. Comparison of the coefficients of absorption of the geometry *2D PASC LUMEN* stimulated either in the Ox or in the Oy direction, for different radii of the fibres and for *d=2cm*.

4.3 Coefficient of absorption and thickness of the material

After having highlighted the effects of the radii of the fibres on the coefficient of absorption at constant porosity for *d=2cm*, the next step consists of studying the evolution of A(ω) when the thickness *d* changes for the geometry *2D PASC LUMEN* stimulated along *Ox*. For two constant frequencies f=400Hz (Figure 10), and f=5000Hz (Figure 11), the evolution of A(ω) for increasing thicknesses between *1mm* and *1m* was studied for each radius R_F. Thus, we can see that A(ω) globally increases when the material is thicker. However, for each radius there exists a critical thickness for which the asymptotic coefficient of absorption is reached[14]. This results show that additional material would be unnecessary beyond this thickness, which is interesting from an economical point of view.

When the frequency increases, all the coefficients of absorption globally increase and the critical frequency decreases for each value of R_F. However, the reverse trend is observed for medium fibres with R_F=80µm, which absorb less energy than larger fibres with R_F=200µm for thicker samples, when *d=60cm* for instance on Figure 10 at f=400Hz. Finally, the acoustic properties at constant frequency of thick material are mainly influenced by the large fibres, which better absorb than small ones. For thinner samples, medium fibres better absorb than larger one, and the overlap of the boundary layers limits the performances of the smaller fibres.

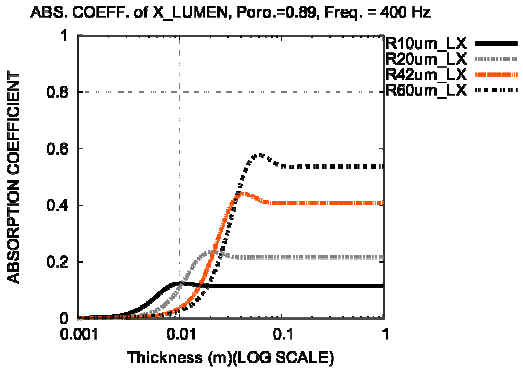

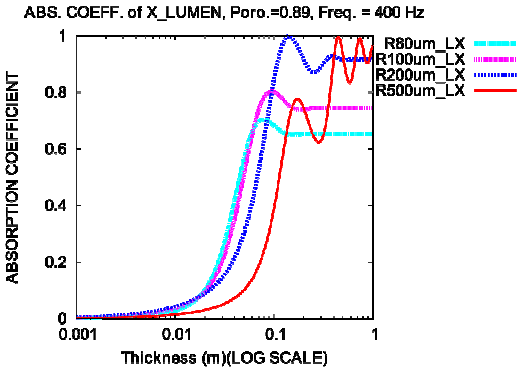

Figure 10. Evolution of the coefficient of absorption for different thicknesses of material at f = 400 Hz, for different radii of the fibres of the geometry *2D PASC LUMEN* stimulated orthogonally to their lumen.

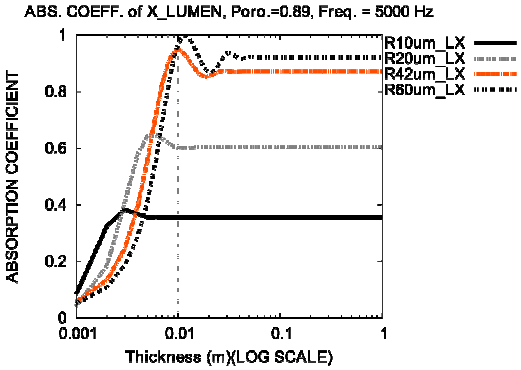

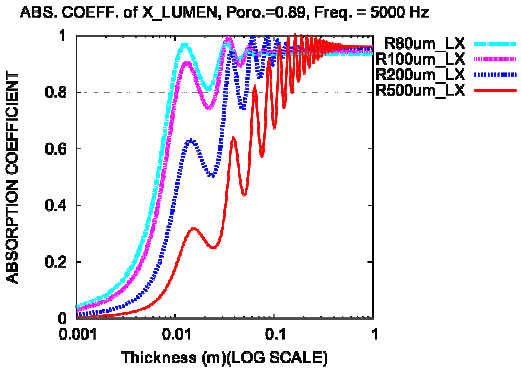

Figure 11. Evolution of the coefficient of absorption for different thicknesses of material at f = 5000 Hz, for different radii of the fibres of the geometry *2D PASC LUMEN* stimulated orthogonally to their lumen.

5. Conclusions

COMSOL Multiphysics is a very useful tool to model the thermo-acoustic properties of fibrous media at the microscopic scale. Our results illustrate to what extent estimating the relationships between the radii of the fibres, the thickness of the material and the coefficient of sound absorption, brings a useful insight towards optimizing the acoustic properties of sound insulating fibrous media.

6. Acknowledgements

We gratefully acknowledge the Agence Nationale de la Recherche (ANR) for financially supporting the Silent Wall project in which this study takes place. Moreover, we are thankful to Bernard Castagnède, Claude Depollier and Olivier Dazel (LAUM, Laboratoire d'Acoustique de l'Université du Maine, Le Mans, France) for bringing their expert's point of view in acoustics. Finally we are thankful to Stephan Savarese (COMSOL France) for his advices and for having provided us the "thermo-acoustics" template model of COMSOL Multiphysics.

7. References

1. J. F. Allard, *Propagation of Sound in Porous Media*. Chapman & Hall, London (1993)

2. J. L. Auriault, "Dynamic behaviour of a porous media saturated by a Newtonian fluid", *Int. J. Engng. Sci.* **18(6)**, 775-785 (1980)

3. J. L. Auriault, L. Borne, and R. Chambon, "Dynamics of porous saturated media, checking of the generalized law of Darcy", *J. Acoust. Soc. Am*. **77(5)**, 1641-1650 (1985)

4. C. Boutin, P. Royer, and J. L. Auriault, "Acoustic absorption of porous surfacing with dual porosity," *Int. J. Solids Struct.* **35(34-35)**, 4709-4737 (1998)

5. Y. Champoux and J. F. Allard, "Dynamic tortuosity and bulk modulus in air-saturated porous media", *J. Appl. Phys.* **70(4)**, 1975-1979 (1991)

6. S. Gasser, F. Paun, and Y. Bréchet, "Absorptive properties of rigid porous media: Application to face centered cubic sphere packing", *J. Acoust. Soc. Am.* **117**, 2090-2099 (2005)

7. D. L. Johnson, J. Koplik, and R. Dashen, "Theory of dynamic permeability and tortuosity in fluid-saturated porous media", *J. Fluid Mech.* **176**, 379-402 (1987)

8. D. Lafarge, "Propagation du son dans les matériaux poreux à structure rigide saturés par un fluide viscothermique", Ph.D. thesis, Université du Maine, (1993)

9. C. Y. Lee, M. J. Leamy and J. H. Nadler, "Numerical Calculation of Effective Density and Compressibility Tensors in Periodic Porous Media: A Multi-Scale Asymptotic Method", Proceedings of the COMSOL Conference 2008, 9 th -11th October; Boston, USA (2008)

10. C. Y. Lee, M. J. Leamy and J. H. Nadler, "Acoustic absorption calculation in irreductible porous media: A unified computational approach", *J. Acoust. Soc. Am.* **126(4)**, 1862-1870 (2009)

11. C. Perrot, F. Chevillotte, and R. Panneton, "Bottom-up approach for microstructure optimization of sound absorbing materials," *J. Acoust. Soc. Am.* **124**, 940-948 (2008)

12. C. Peyrega, D. Jeulin, C. Delisée and J. Malvestio, "3D morphological modelling of a random fibrous network" *Image Anal. Stereol.* **28**, 129-141 (2009)

13. C. Peyrega, D. Jeulin, C. Delisée and J. Malvestio, "3D morphological characterization of phonic insulation fibrous media" *Adv. Eng. Mat.* Accepted article to be published (2010)

14. J. Pfretzschner and R. M. Rodriguez, "Acoustical absorption and critical thickness", Proceedings of the 17th International Congress of Acoustics (ICA) 2001, 2nd-7th September; Rome, Italy (2001)

15. S. R. Pride, F. D. Morgan, and A. F. Gangi, "Drag forces of porous medium acoustics", *Phys. Rev. B* **47**, 4964 (1993)

16. E. Sanchez-Palencia, *Non-Homogeneous Media and Vibration Theory Media*, Springer-Verlag, Heidelberg, (1980)

17. R. Venegas and O. Umnova, "On the influence of the micro-geometry on sound propagation through periodic array of cylinders", Proceedings of the Conference Acoustics 08, 29th June-4th July; Paris, France, 807-812 (2008)